ERASMUS MUNDUS MASTER OF MECHANICAL ENGINEERING

MEMOIRE-THESIS

Ze ZHOU

Acoustic particle velocity measurement by ultra-light membrane and its applications in acoustic holography

June 2007

INSTITUT NATIONAL DES SCIENCES APPLIQUEES DE LYON - FRANCE
ESCOLA TÈCNICA SUPERIOR D'ENGINYERIA INDUSTRIAL DE BARCELONA, UNIVERSITAT POLITÈCNICA DE CATALUNYA - ESPAGNE
THE COLLEGE OF THE HOLY AND UNDIVIDED TRINITY OF QUEEN ELIZABETH NEAR DUBLIN - IRLANDE

Declaration

I declare that I am the sole author of this dissertation and that the work presented in it, unless otherwise referenced, is my own. I also declare that the work has not been submitted, in whole or in part, to any other university or college for a degree or other qualification.

I authorize the library of Trinity College Dublin to lend or copy this dissertation on request.

Abstract

Acoustic holography is a non-destructive method used to determine the spatial propagation of acoustical waves. Conventionally, the acoustic holography measures the acoustic pressure. Until recently, a very limited number of techniques to measure the acoustic particle velocity have been introduced.

The Laboratory of Vibration and Acoustics of INSA de Lyon, France has recently developed a novel method to directly measure the acoustic velocity field by a light membrane, with the assistance of a laser vibrometer.

Theories allowing getting acoustic pressure and acoustic power from particle velocity have also been developed.

The primary goal of this project is to apply the recently developed theories to a series of acoustic measurements. The objectives consist of the validation of the method and the evaluation of its performances under various circumstances.

In several experiments, results obtained by the approach of membrane’s measurement are compared with results from conventional microphone’s measurement and a relatively new P-U probe measurement.

Acknowledgements

I would like to thank to Professor Bernard Laulagnet for his guidance throughout this project; Quentin Leclère for his patient assistance and Frédérique for his generous helps.

Thanks to Laboratoire Vibrations Acoustique of INSA de Lyon for providing me an amicable research environment.

I would like thank also to Professor Henry Rice of Trinity College, Dublin for leading me into acoustics.

Last but not least, many thanks to the Erasmus Mundus program which allowed me to study in Europe and wish this program a greater future success.

Table of Contents

Declaration i

Abstract ii

Acknowledgments iii

Contents iv

1.0 Introduction 1
1.1 Acoustic holography 1
1.1.1 Basic concept 1
1.1.2 Far-field, Near-field and newly developed acoustic holography methods 2
1.2 Measurement of acoustic quantities and their acoustic holography applications 4
1.2.1 Acoustic pressure measurement 4
1.2.2 Acoustic intensity measurement 4
1.2.3 Particle velocity measurement 4
1.2.4 Applications in acoustic holography 5
1.3 Using a light membrane to measure the acoustic particle velocity 6
1.4 Objectives of the project 7

2.0 Theories 8
2.1 Fourier series and Fourier transform 8
2.1.1 Fourier series with complex coefficients 8
2.1.2 Fourier transform and Discrete Fourier transform 9
2.1.3 FFT and its realization in Matlab 10
2.2 Application of Fourier transform into Helmholtz equation 11
2.2.1 Fourier transform of the Helmolts equation 11
2.2.2 Propagative and Evanescent wave 13
2.2.3 From velocity to pressure 14
2.3 Membrane theory 16
2.3.1 Membrane governing equations 16
2.3.2 Mass correction 17
2.4 Procedure of the calculations 20
2.4.1 Filter of measured velocity by the membrane 20
2.4.2 Getting velocity and pressure field 22
2.4.3 Sound power 23

3.0 Experiments 24

3.1 Preparation of the membranes 24
3.1.1 Material 24
3.1.2 Frame and adhesion 24
3.1.3 Membrane with added mass 25
3.1.4 Conclusion of the membrane realizations 26
3.2 Data acquisition by the vibrometer 27
3.2.1 The vibrometer system 27
3.2.2 Acquisition parameters 28
3.3 Experiments and rigs 29
3.3.1 Experiments in an anechoic room 29
3.3.2 Experiments in front of a vibrating plate 31
3.3.3 Experiment to measure a motor’s noise 33

4.0 Results 35
4.1 Results of the experiments with the vibrating plate 35
4.1.1 Measured velocity field by membrane and its pressure field 35
4.1.2 Filtered velocity field and its pressure field 40
4.1.3 Corrected velocity field and pressure field of a heavy membrane 43
4.1.4 Comparison with Microflown results 46
4.1.5 Validation of evanescent wave 47
4.2 Results in the anechoic room 49
4.3 Results of the motor’s noise 52

5.0 Discussions 54
5.1 Evaluations of results 54
5.2 Recommended future works 55

6.0 References 56

1.0 Introduction

1.1 Acoustic holography

1.1.1 Basic concept

1.1.2 Far-field, Near-field and newly developed acoustic holography methods

1.2 Measurement of acoustic quantities and their acoustic holography applications

1.2.1 Acoustic pressure measurement

1.2.2 Acoustic intensity measurement

1.2.3 Particle velocity measurement

1.2.4 Applications in acoustic holography

1.3 Using a light membrane to measure the acoustic particle velocity

1.4 Objectives of the project

1.0 Introduction

1.1 Acoustic holography

1.1.1 Basic concept

Acoustic holography, invented by Dennis Gabor in 1948, is a method used to determine the spatial propagation of acoustical waves, or for detecting acoustic sources or objects by measuring acoustic parameters away from the source. It is a non-destructive testing technique which produces a visual image of the internal structure of the part being examined [1].

Measuring techniques included within acoustic holography are becoming increasingly popular in various fields, most notably those of transportation, vehicle and aircraft design, and NVH (Noise, Vibration, and Harshness).

Figure 1.1 shows acoustic holography of a cooling fan.

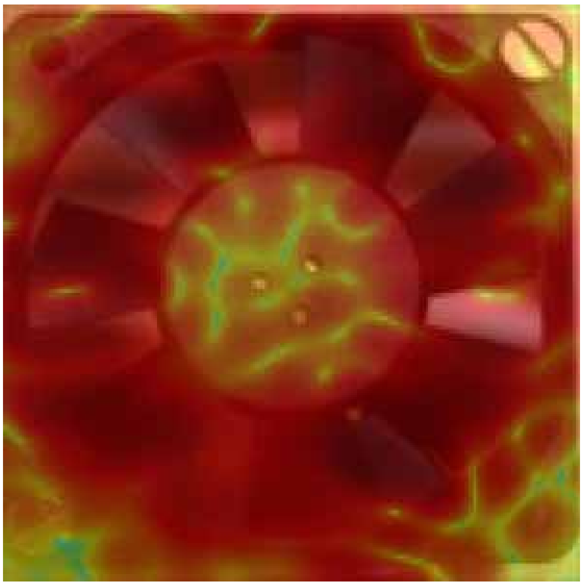

Figure 1.1 Acoustic holography of a cooling fan
From http://www.acoustic-holography.com

1.1.2 Far-field, Near-field and newly developed acoustic holography methods

Two distinct forms of acoustical holography exist, far-field acoustical holography and near-field acoustical holography.

In far-field acoustical holography (FAH), the hologram is recorded far from the source. Compared to Near-field acoustic holography (NAH), the technique of FAH has received less attention because of the fact that it can not capture the information of short wavelength or subsonic surface data that does not radiate to far field [2].

However, a study of the applications of far-field acoustic holography on circular cylindrical surfaces by Williams and Norris [3] showed high accurate imaging of FAH.

Near-field acoustic holography, invented by E. G. Williams and J. D. Maynard [4] in 1980 is generally preferred in the sense that it includes information about the evanescent, subsonic pressure field which does not radiate to the far field.

NAH has been widely used in the automotive industry to study interior noise and tire noise, in musical acoustics to study vibration and radiation of violin-family instruments, and in the aircraft industry to study interior cabin noise and fuselage vibrations. Applications are also found in underwater acoustics, especially in studies of vibration, radiation, and scattering from ships and submarines.

As a variant of NAH, the Statistical optimized near-field acoustic holography (SONAH) was developed by Steiner and Hald [5],[6]. The advantage of this method is to avoid the finite spatial transforms utilized by conventional NAH and thus the problem of truncation errors of the transforms.

NAH in automotive and naval applications can yield a resolution in the order of one centimeter. In a recent paper, Scholte et al. [7] reported a high resolution NAH measurement with a carefully tuned acoustic signal processing and measurement set-up. Their measurements showed that the sources are identified with sub-millimeter resolution.

More recently, a novel near-field acoustic holography (NFAH) technique which combines the nanometer-scale spatial resolution of the conventional scanning probe microscope (SPM) with the surface and subsurface imaging capabilities was proposed by Shekhawat et al [8]. This technique allows detecting structure in the nanometer scale (Fig 1.2).

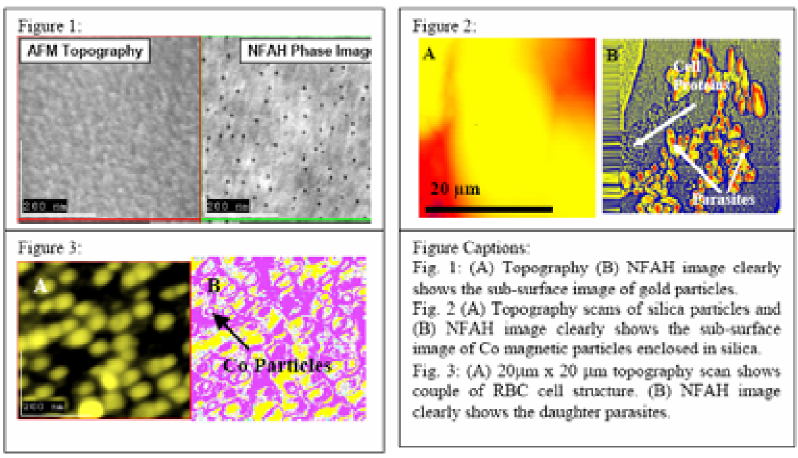

Figure 1.2 Near-field acoustic holography shows nanometer scale

1.2 Measurement of acoustic quantities and their acoustic holography applications

1.2.1 Acoustic pressure measurement

Acoustic pressure is measured by an acoustic pressure sensor [9]. A pressure sensor is generally called a microphone. In essence, a microphone is a pressure transducer adapted for the transduction of sound waves over a broad spectral range. For the perception of air waves or vibrations in solids, the sensor is called a microphone, while for the operation in liquids, it is called a hydrophone. Microphone and hydrophone have the same basic structure as a pressure sensor: it is comprised of a moving diaphragm and a displacement sensor which converts the diaphragm's deflections into an electrical signal.

1.2.2 Acoustic intensity measurement

Acoustic intensity can be measured by acoustic intensity probe (or sound intensity probe).

1.2.3 Particle velocity measurement

The acoustic field is difficult to measure directly and up to these last years, no velocity sensors existed.

One way to get the velocity information is by indirect measurement, via an intensity probe, and uses the spatial finite difference approximation given by the two microphones of the intensity probes [10].

In recent years, a new technique to directly measure the particle velocity using a hot wire was developed. This method uses a new device named Microflown [11], [12].

1.2.4 Applications in acoustic holography

Acoustic holography is usually based on the measurement of sound pressure. Typically, temporal acoustic data are acquired by measurement with a single microphone which scans an imaginary two-dimensional surface. In some cases, an array of microphones is used and the pressure is measured instantaneously by the array.

Figure 1.3 96 high-precision microphones combined on an array and connected to an analyzer. From [13]

In recent years, as proposed and carried out by Finn et al. [14], [15], the acoustic particle velocity can also be measured by an array of sound intensity probe: *p-u* sound intensity probe produced by Microflown. The performance of the latter is reported to be better than that of the conventional pressure measurement, particularly when the sound pressure is predicted close to the source. Acoustic holography based on the particle velocity is also less sensitive to transducer mismatch than the conventional technique based on the pressure.

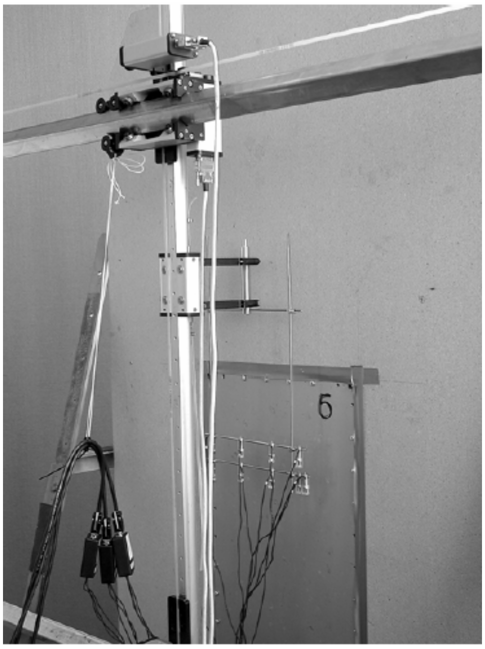

Figure 1.4 The Microflown array in front of the steel panel in the baffle From [15]

1.3 Using a light membrane to measure the acoustic particle velocity

Recently, Leclère et al [16] proposed a new method for acoustic particle velocity field measurement by using an ultra light membrane and a laser beam. The main advantage of this method is its high spatial resolution of the image and its ease to realize.

The velocity of the membrane in acoustic field is measured by a vibrometer to estimate the acoustic particle velocity. The membrane is fixed on a frame and ideally without tension in order to avoid inaccuracy of measurement caused the excited membrane modes.

In the cases that the membrane's mass cannot be neglected, a mass correction technique can take the mass effect into account and retrieve the acoustic velocity without the presence of the membrane. This technique is based on the infinite membrane vibration theory, summarized by Jenkins and Korde in their paper [17].

In low frequency range, a relatively heavier membrane (100g/ m^2) is reported to have better performance than a lighter one (10g/ m^2) in characterizing the acoustic field.

1.4 Objectives of the project

Previous works by Leclère et al have demonstrated the capability of the membrane method, in measuring acoustic particle velocities.

The purpose of this project is to do further studies and researches concerning the theories and techniques of the membrane's measurement. Objectives are proposed in several aspects. They are:

- Development of theory that can get acoustic pressure and acoustic power based on measured particle velocity.
- Comparison of differently made membranes in measurements.
- Comparison of results from membrane measurements with results from conventional measurements. The compared results are velocity, pressure and sound power.

To fulfill the purpose, a series of experiments are carried out. They are:

- Experiments in an anechoic room.
- Experiments in front of a vibrating plate
- Experiment to measure a motor's noise

2.0 Theories

2.1 Fourier series and Fourier transform

2.1.1 Fourier series with complex coefficients
2.1.2 Fourier transform and Discrete Fourier transform
2.1.3 FFT and its realization in Matlab

2.2 Application of Fourier transform into Helmholtz equation

2.2.1 Fourier transform of the Helmolts equation
2.2.2 Propagative and Evanescent wave
2.2.3 From velocity to pressure

2.3 Membrane theory

2.3.1 Membrane governing equations
2.3.2 Mass correction

2.4 Procedure of the calculations

2.4.1 Filter of measured velocity by the membrane
2.4.2 Getting velocity and pressure field
2.4.3 Sound power

2.0 Theories

2.1 Fourier series and Fourier transform

2.1.1 Fourier series with complex coefficients

Consider a function $f(x)$, which is periodic in $\left[-L/2, L/2\right]$. It can be expressed by Fourier series with complex coefficients.

$$f(x) = \sum_{n=-\infty}^{\infty} A_n e^{j2\pi nx/L} \tag{2.1}$$

$$A_n = \frac{1}{L}\int_{-L/2}^{L/2} f(x) e^{-j2\pi nx/L} \mathrm{d}x \tag{2.2}$$

where $f(x)$ and A_n are all complexes. Equation (2.1) shows that $f(x)$ is the sum of harmonic functions with different frequencies. A_n gives the information on the positive (n > 0) and negative (n < 0) frequencies of the function $f(x)$.

2.1.2 Fourier transform and Discrete Fourier transform

The Fourier transform is a generalization of the Complex Fourier series at the limit when the period of the function $f(x)$ approaches to infinite.

The Fourier transform pair is,

$$f(x) = \int_{-\infty}^{\infty} F(k) e^{j2\pi kx} \mathrm{d}k \tag{2.3}$$

$$F(k) = \int_{-\infty}^{\infty} f(x) e^{-j2\pi kx} \mathrm{d}x \tag{2.4}$$

$f(x)$ and $F(k)$ represent the same physical term, but in a different representation. When we consider $f(x)$, the representative point is in the amplitude – time domain. When we consider $F(k)$, the representative point is in the amplitude – frequency domain.

The conditions for that a function $f(x)$ to have a Fourier transform is that,

1. The function $f(x)$ is limited (with no infinite values).

2. The integration of $|f(x)|$ between ($-\infty, \infty$) have a finite value.

3. The number of the discontinuities of $f\left(x\right)$ is finite.

When the function $f\left(x\right)$ is not continuous or only discrete point values are available, Discrete Fourier transform is used instead of the continuous Fourier transform. The Discrete Fourier transform pair is

$$f_k = \frac{1}{N}\sum_{n=0}^{N-1} F_n e^{j2\pi nk/N} \tag{2.5}$$

$$F_n = \sum_{k=0}^{N-1} f_k e^{-j2\pi nk/N} \tag{2.6}$$

where $f_k = f(x_k)$ and $x_k = k\Delta$, with Δ to be the discrete step of *x*.

2.1.3 FFT and its realization in Matlab

In this thesis, all Fourier transforms are calculated by a Fast Fourier transform (FFT) algorithm.

The fast Fourier transform (FFT) is a Discrete Fourier transform algorithm which reduces the number of computations needed for N points from $2N^2$ to $2N\lg N$.

In practice, the FFT calculations are done with Matlab. The results obtained by Matlab are slightly different from those obtain by equation (2.5) and (2.6).

In Matlab, f_k and F_n are

$$f_k = \sum_{n=0}^{N-1} F_n e^{j2\pi nk/N} \tag{2.7}$$

$$F_n = \frac{1}{N}\sum_{k=0}^{N-1} f_k e^{-j2\pi nk/N} \tag{2.8}$$

2.2 Application of Fourier transform into Helmholtz equation

2.2.1 Spatial Fourier transform of the Helmholtz equation

In a three dimensional coordinate, the direction of an acoustic wave propagation is along the z axis. A two dimensional spatial Fourier transform (in the plan x-y) of acoustic pressure $\overline{p}$ can be applied, and gives the transform pair

$$\tilde{p}_{mn}(z) = \frac{1}{l_x l_y}\int_0^{l_x}\int_0^{l_y} \overline{p}_z\left(x,y,z\right) e^{-jmx 2\pi / l_x} e^{-jny 2\pi / l_y} \mathrm{d}x\mathrm{d}y \tag{2.9}$$

$$\overline{p}_z\left(x,y,z\right) = \sum_{m=0}^{M-1}\sum_{n=0}^{N-1} \tilde{p}_{mn}(z) e^{jmx 2\pi / l_x} e^{jny 2\pi / l_y} \tag{2.10}$$

where $\overline{p}_z\left(x,y,z\right)$ is the time independent acoustic pressure in the spatial domain, and $\tilde{p}_{mn}(z)$ is the spatial transforms. l_x and l_y are the lengths of the membrane in x and y directions.

The acoustic particle velocity can be Fourier transformed in the same manner

$$\tilde{v}_{mn}(z) = \frac{1}{l_x l_y}\int_0^{l_x}\int_0^{l_y} \overline{v}_z\left(x,y,z\right) e^{-jmx 2\pi / l_x} e^{-jny 2\pi / l_y} \mathrm{d}x\mathrm{d}y \tag{2.11}$$

$$\overline{v}_z\left(x,y,z\right) = \sum_{m=0}^{M-1}\sum_{n=0}^{N-1} \tilde{v}_{mn}(z) e^{jmx 2\pi / l_x} e^{jny 2\pi / l_y} \tag{2.12}$$

Now consider the acoustic governing equation: Helmholtz equation,

$$\Delta\overline{p} + k^2\overline{p} = 0 \tag{2.13}$$

Its form in the three dimensional coordinate is,

$$\frac{\partial^2 \overline{p}}{\partial x^2} + \frac{\partial^2 \overline{p}}{\partial y^2} + \frac{\partial^2 \overline{p}}{\partial z^2} + k^2\overline{p} = 0 \tag{2.14}$$

where $\bar{p}$ is the acoustic pressure, and k is the wave number corresponding to a frequency f, with the following relation

$$k = \frac{\omega}{c} = \frac{2\pi f}{c} \tag{2.15}$$

where ω is the angular frequency and c is the sound speed.

Bring equation (2.10) into equation (2.14), the pressure terms in the Helmholtz equation are expressed by their Fourier transforms

$$\begin{aligned} &\sum_{m=0}^{M-1}\sum_{n=0}^{N-1} \tilde{p}_{mn}(z)\left(-\frac{4\pi^2 m^2}{{l_x}^2} - \frac{4\pi^2 n^2}{{l_y}^2}\right) e^{jmx2\pi/l_x} e^{jny2\pi/l_y} \\ &+\sum_{m=0}^{M-1}\sum_{n=0}^{N-1} \frac{\partial^2 \tilde{p}_{mn}(z)}{\partial z^2} e^{jmx2\pi/l_x} e^{jny2\pi/l_y} \\ &+\sum_{m=0}^{M-1}\sum_{n=0}^{N-1} k^2 \tilde{p}_{mn}(z) e^{jmx2\pi/l_x} e^{jny2\pi/l_y} \\ &= 0 \end{aligned} \tag{2.16}$$

So

$$\frac{\partial^2 \tilde{p}_{mn}(z)}{\partial z^2} + \left(k^2 - \frac{4\pi^2 m^2}{{l_x}^2} - \frac{4\pi^2 n^2}{{l_y}^2}\right)\tilde{p}_{mn}(z) = 0 \tag{2.17}$$

Equation (2.17) is the Fourier transformed Helmholtz equation. The wave number term is replaced by a the reduced wave number k_{mn}^z, with the relation

$$k_{mn}^z = \sqrt{k^2 - \frac{4\pi^2 m^2}{{l_x}^2} - \frac{4\pi^2 n^2}{{l_y}^2}} \tag{2.18}$$

So the Fourier transformed Helmholtz equation becomes

$$\frac{\partial^2 \tilde{p}_{mn}(z)}{\partial z^2} + \left(k_{mn}^z\right)^2 \tilde{p}_{mn}(z) = 0 \tag{2.19}$$

The form of the solution to equation (2.17) and (2.19) is

$$\tilde{p}_{mn}(z) = \tilde{p}_{mn} e^{-jk_{mn}^{z} z} \tag{2.20}$$

for propagation in the positive *z* direction, and

$$\tilde{p}_{mn}(z) = \tilde{p}_{mn} e^{jk_{mn}^{z} z} \tag{2.21}$$

for propagation in the negative *z* direction.

Since the acoustic particle velocity is also governed by the Helmholtz equation, in the same manner, we have the Helmholtz equation for the spatial transformed acoustic particle velocity,

$$\frac{\partial^2 \tilde{v}_{mn}(z)}{\partial z^2} + \left(k_{mn}^{z}\right)^2 \tilde{v}_{mn}(z) = 0 \tag{2.22}$$

Its solutions are the same forms as (2.20) and (2.21).

2.2.2 Propagative and Evanescent wave

A propagative wave can propagate without any decay.

An evanescent wave is a nearfield wave exhibiting exponential decay with distance.

These propagative or evanescent properties can be determined by k_{mn}^{z}. Take equation (2.18), k_{mn}^{z} can be expressed as

$$k_{mn}^{z} = \sqrt{k^2 - \frac{4\pi^2 m^2}{l_x^{\ 2}} - \frac{4\pi^2 n^2}{l_y^{\ 2}}}$$

$$= \begin{cases} \sqrt{k^2 - \frac{4\pi^2 m^2}{l_x^{\ 2}} - \frac{4\pi^2 n^2}{l_y^{\ 2}}}, (k^2 \geq \frac{4\pi^2 m^2}{l_x^{\ 2}} + \frac{4\pi^2 n^2}{l_y^{\ 2}}) \\ \pm j\sqrt{\left| k^2 - \frac{4\pi^2 m^2}{l_x^{\ 2}} - \frac{4\pi^2 n^2}{l_y^{\ 2}} \right|}, (k^2 < \frac{4\pi^2 m^2}{l_x^{\ 2}} + \frac{4\pi^2 n^2}{l_y^{\ 2}}) \end{cases} \tag{2.23}$$

When k_{mn}^{z} is real, the acoustic wave is propagative, and when k_{mn}^{z} is complex, the acoustic wave is evanescent.

When $k_{mn}^{z} = 0$, the Helmholtz equation becomes

$$\frac{\partial^2 \tilde{v}_{mn}(z)}{\partial z^2} = 0 \quad \text{and} \quad \frac{\partial^2 \tilde{p}_{mn}(z)}{\partial z^2} = 0 \tag{2.24}$$

To satisfy the conditions that the acoustic pressure and velocity have limit at far field, the only solution to this case is

$$\tilde{v}_{mn}(z) = 0 \quad \text{and} \quad \tilde{p}_{mn}(z) = 0 \tag{2.25}$$

2.2.3 From velocity to pressure

Take the relation between the spatial derivative of acoustic pressure and the time derivative of the particle velocity (Euler equation)

$$\frac{\partial \overline{p}_z}{\partial z} = -\rho_0 \frac{\partial \overline{v}_z}{\partial t} \tag{2.26}$$

where ρ_0 is air density.

The harmonic nature with time of the sound wave gives the relation,

$$\frac{\partial \overline{v}_z}{\partial t} = j\omega \overline{v}_z \tag{2.27}$$

So equation (2.26) becomes,

$$\frac{\partial \overline{p}_z}{\partial z} = -j\omega \rho_0 \overline{v}_z \tag{2.28}$$

The spatial Fourier transform of equation (2.28) gives

$$\frac{\partial \tilde{p}_{mn}}{\partial z} = -j\omega \rho_0 \tilde{v}_{mn} \tag{2.29}$$

Take the spatial derivative in the *z* direction of equation (2.29),

$$\frac{\partial^2 \tilde{p}_{mn}}{\partial z^2} = -j\omega \rho_0 \frac{\partial \tilde{v}_{mn}}{\partial z} \tag{2.30}$$

Bring equation (2.30) into the transformed Helmholtz equation (2.19)

$$\tilde{p}_{mn} = \frac{j\omega \rho_0 \, {\partial \tilde{v}_{mn}}/{\partial z}}{\left(k_{mn}^z\right)^2} \tag{2.31}$$

From the transformed Helmholtz equation of velocity: equation (2.22), we can write the relation between the spatial derivative of velocity and the velocity which propagates in the positive *z* direction

$$\frac{\partial \tilde{v}_{mn}}{\partial z} = -jk_{mn}^z \tilde{v}_{mn} \tag{2.32}$$

Finally, equation (2.31) and (2.32) together give the relation between transformed pressure and transformed velocity

$$\tilde{p}_{mn} = \frac{\omega\rho_0\tilde{v}_{mn}}{k_{mn}^z} \tag{2.33}$$

Therefore, the acoustic impedance in the transformed domain is $\frac{\omega\rho_0}{k_{mn}^z}$ in stead of $\frac{\omega\rho_0}{k}$.

2.3 Membrane theory

2.3.1 Membrane governing equation

Consider an infinite membrane located in the plane z = 0. An acoustic wave travels along the z axis. When it reaches the membrane, a transmitted wave goes through the membrane and a reflected travels back. (Fig 2.1)

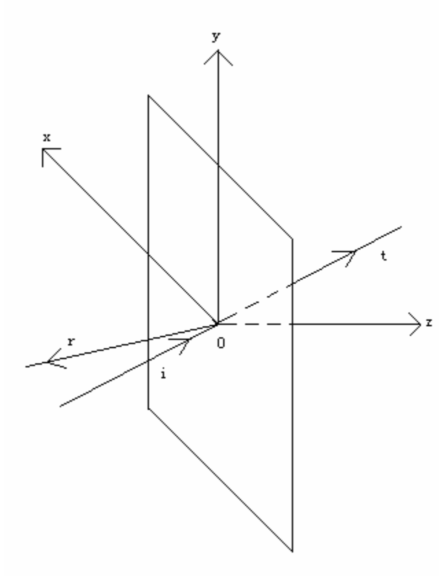

Figure 2.1 Schematic acoustic waves (incident, transmitted and reflected) and the membrane

The governing equation is [16],

$$\rho h \frac{\partial^2 u_z(x,y,t)}{\partial t^2} = T\nabla^2 u_z(x,y,t) + p^i(x,y,0,t) + p^r(x,y,0,t) - p^t(x,y,0,t) \quad (2.34)$$

where ρh denotes the membrane mass per unit area (with ρ denoting the membrane density and h its thickness), T the uniform tension in the membrane, $u_z(x,y,t)$ the membrane displacement in the Z direction at point (x , y) and at time t, and p^i, p^r and p^t, the transmitted, incident and reflected acoustic pressure, respectively.

A practical simplification to equation (2.34) can be done by neglecting the uniform tension T in the membrane. The main reason of the simplification is that when a membrane is mounted in a framework, with particular technique, the tension can be controlled to be very small. Another reason is that the exact tension can be very hardly measured.

In the following chapters, the tension term will be discussed. We will compare the results obtained by the fully adhered membrane – high tension and the partially adhered membrane – low tension. Therefore to simplify the theory part, we neglect the tension term. The governing equation then becomes,

$$\rho h \frac{\partial^2 u_z(x,y,t)}{\partial t^2} = p^i(x,y,0,t) + p^r(x,y,0,t) - p^t(x,y,0,t) \qquad (2.35)$$

2.3.2 Mass correction

Ideally, if the membrane has no mass, the measured velocity of the membrane will be the acoustic particle velocity in the absence of the membrane. When the mass of the membrane can not be neglected, a mass correction must be applied in order to calculate the acoustic particle velocity from the measured membrane velocity.

In this part, the equation of mass correction will be established.

Bring equation (2.20) and (2.21) back into equation (2.10), we have the time independent Fourier transforms for the transmitted, incident and reflected acoustic pressure, respectively.

$$\bar{p}_z^i\left(x,y,z\right)=\sum_{m=0}^{M-1}\sum_{n=0}^{N-1}\tilde{p}_{mn}^i e^{-jk_{mn}^z z} e^{jmx2\pi/l_x} e^{jny2\pi/l_y} \tag{2.36}$$

$$\bar{p}_z^r\left(x,y,z\right)=\sum_{m=0}^{M-1}\sum_{n=0}^{N-1}\tilde{p}_{mn}^r e^{jk_{mn}^z z} e^{jmx2\pi/l_x} e^{jny2\pi/l_y} \tag{2.37}$$

$$\bar{p}_z^t\left(x,y,z\right)=\sum_{m=0}^{M-1}\sum_{n=0}^{N-1}\tilde{p}_{mn}^t e^{-jk_{mn}^z z} e^{jmx2\pi/l_x} e^{jny2\pi/l_y} \tag{2.38}$$

For the membrane displacement,

$$\bar{u}_z\left(x,y\right)=\sum_{m=0}^{M-1}\sum_{n=0}^{N-1}\tilde{u}_{mn} e^{jmx2\pi/l_x} e^{jny2\pi/l_y} \tag{2.39}$$

The harmonic nature in time of acoustic allows us to write

$$p^n\left(x,y,0,t\right)=\bar{p}^n\left(x,y,0\right)e^{j\omega t} \quad \text{(n=j, r, t)} \tag{2.40}$$

$$u_z\left(x,y,0,t\right)=\bar{u}_z\left(x,y,0\right)e^{j\omega t} \tag{2.41}$$

The membrane governing equation (2.35) becomes in its Fourier transformed form

$$\begin{aligned}&-\omega^2\rho h\sum_{m=0}^{M-1}\sum_{n=0}^{N-1}\tilde{u}_{mn} e^{jmx2\pi/l_x} e^{jny2\pi/l_y} \\ &=\sum_{m=0}^{M-1}\sum_{n=0}^{N-1}\left(\tilde{p}_{mn}^i+\tilde{p}_{mn}^r-\tilde{p}_{mn}^t\right)e^{jmx2\pi/l_x} e^{jny2\pi/l_y}\end{aligned} \tag{2.42}$$

Hence

$$-\omega^2 \rho h \tilde{u}_{mn} = \tilde{p}^i_{mn} + \tilde{p}^r_{mn} - \tilde{p}^t_{mn} \tag{2.43}$$

Take the Fourier transformed Euler equation

$$-j\omega\rho_0\tilde{v}_{mn} = \frac{\partial \tilde{p}_{mn}}{\partial z} \tag{2.44}$$

Where $\tilde{v}_{mn}$ can be expressed by

$$\tilde{v}_{mn} = \frac{\partial \tilde{u}_{mn}}{\partial t} = j\omega\tilde{u}_{mn} \tag{2.45}$$

On the transmitted side of the membrane, we then have

$$\rho_0\omega^2\tilde{u}_{mn} = -jk^z_{mn}\tilde{p}^t_{mn} \tag{2.46}$$

And on the incident side of the membrane,

$$\rho_0\omega^2\tilde{u}_{mn} = jk^z_{mn}\left(\tilde{p}^r_{mn} - \tilde{p}^i_{mn}\right) \tag{2.47}$$

Combine equation (2.43), (2.46) and (2.47) together, we have

$$\tilde{u}_{mn} = \frac{-2jk^z_{mn}\tilde{p}^i_{mn}}{jk^z_{mn}\omega^2\rho h + 2\omega^2\rho_0} \tag{2.48}$$

And the velocity

$$\tilde{v}_{mn} = j\omega\tilde{u}_{mn} = \frac{2k^z_{mn}\tilde{p}^i_{mn}}{jk^z_{mn}\omega\rho h + 2\omega\rho_0} \qquad (2.49)$$

Now we consider the velocity component $\overline{v}^{ac}$, in the absence of the membrane.

In this situation the incident wave does not change from the previous case. Equation (2.33) becomes

$$\tilde{v}^{ac}_{mn} = \frac{\tilde{p}^i_{mn}}{\rho_0\omega / k^z_{mn}} \qquad (2.50)$$

Combining equation (2.49) and equation (2.50), we have

$$\tilde{v}^{ac}_{mn} = \tilde{v}_{mn}\left(1 + \frac{jk^z_{mn}\rho h}{2\rho_0}\right) \qquad (2.51)$$

Equation (2.51) performs the mass correction to get the real velocity in the absence of the membrane, by multiplying a factor to the Fourier transformed acoustic velocity obtained by the membrane.

2.4 Procedure of the calculations

2.4.1 Filter of measured velocity by the membrane

Ideally, if the membrane used for the acquisition has no mass and no interior tension, the measured velocity of the membrane will represent perfectly the propagating acoustic field

However, from the experimental results obtained by the membrane measurement, artifacts in the acoustic field are often observed. The spatial scales of the artifacts are normally smaller than the spatial wave length components in the acoustic holography.

Therefore a filter of the measured velocity can be applied to eliminate those artifacts.

Consider again the spatial Fourier transform of the velocity

$$\overline{v}(x,y)=\sum_{m=0}^{M-1}\sum_{n=0}^{N-1}\tilde{v}_{mn}e^{j2\pi mx/l_x}e^{j2\pi ny/l_y} \tag{2.52}$$

The spatial wave number of the transformed velocity component with index (m, n) is

$$k_{mn}=\sqrt{\left(\frac{2\pi m}{l_x}\right)^2+\left(\frac{2\pi n}{l_y}\right)^2} \tag{2.53}$$

The corresponding spatial wave length is

$$\lambda_{mn}=\frac{2\pi}{k_{mn}} \tag{2.54}$$

The technique of the filter is to eliminate the component of the transformed velocity with a “relatively” short wave length, i.e. to set their corresponding $\tilde{v}_{mn}$ to be zero.

Since the criteria to determine to which extend the component to eliminate depends on each experiment and has no established rules, therefore it is based on an observation basis.

One criterion is that the maximum spatial wave length to eliminate could be as long as the spatial wave length of the real acoustic propagation. Another criterion is that when the acoustic field presents a strip characteristic – horizontal or vertical, the filter factor can be taken bigger.

As frequency increases, the spatial wave length of the acoustic propagation decrease until to a limit that the filter is no longer necessary.

The filtered velocity is

$$\overline{v}^*(x,y) = \sum_{m=0}^{M-1}\sum_{n=0}^{N-1} \tilde{v}^*_{mn} e^{j2\pi mx/l_x} e^{j2\pi ny/l_y} \tag{2.55}$$

where

$$\tilde{v}^*_{mn} = \begin{cases} 0, (\lambda_{mn} < L) \\ \tilde{v}_{mn}, (\lambda_{mn} > L) \end{cases} \tag{2.56}$$

where L depends on the frequency range.

2.4.2 Getting velocity and pressure field

This part is a resume of how to get the velocity and pressure field. The steps to follow are:

- Filter of the measured velocity $\overline{v}^*$, by using equation (2.55).
- Get the Fourier transform of the filtered velocity $\tilde{v}_{mn}$, by using the "fft2" function in Matlab.
- For a heavy membrane, do the mass correction $\tilde{v}^{ac}_{mn}$, by using equation (2.51). For a light membrane $\tilde{v}^{ac}_{mn} = \tilde{v}_{mn}$.
- Get the velocity in absence of the membrane $\overline{v}^{ac}$, by doing the inverse Fourier transform of $\tilde{v}^{ac}_{mn}$, by using "ifft2" function in Matlab.
- Get the Fourier transform of the pressure, by using equation (2.33).
- Get the acoustic pressure $\overline{p}$, by the inverse Fourier transform of $\tilde{p}_{mn}$, by using "ifft2" function in Matlab.

2.4.3 Sound power

Sound power can be calculated by the following equation.

$$W = \frac{1}{2}\int_s \mathrm{Re}\left\{\overline{p}\left(x,y\right)\cdot {}^{*}\overline{v}\left(x,y\right)\right\}\mathrm{d}x\mathrm{d}y \tag{2.57}$$

where ${}^{*}\overline{v}\left(x,y\right)$ is the conjugate of $\overline{v}\left(x,y\right)$.

Equation (2.57) can be expressed by the Fourier transformed pressure and velocity.

$$\begin{aligned} W &= \frac{1}{2}\omega\rho_0\,\mathrm{Re}\int_s \sum_{m=0}^{M-1}\sum_{n=0}^{N-1}\left(\frac{\tilde{v}_{mn}}{k_{mn}^{z}}e^{jmx2\pi/l_x}e^{jny2\pi/l_y}\right)\cdot\sum_{r=0}^{M-1}\sum_{s=0}^{N-1}\left({}^{*}\tilde{v}_{rs}e^{-jrx2\pi/l_x}e^{-jsy2\pi/l_y}\right)\mathrm{d}x\mathrm{d}y \\ &= \frac{1}{2}l_x l_y\omega\rho_0\sum_{m=0}^{M-1}\sum_{n=0}^{N-1}\mathrm{Re}\left(\frac{\tilde{v}_{mn}\cdot{}^{*}\tilde{v}_{mn}}{k_{mn}^{z}}\right) \end{aligned} \tag{2.58}$$

3.0 Experiments

3.1 Preparation of the membranes

3.1.1 Material
3.1.2 Frame and adhesion
3.1.3 Membrane with added mass
3.1.4 Conclusion of the membrane realizations

3.2 Data acquisition by the vibrometer

3.2.1 The vibrometer system
3.2.2 Acquisition parameters

3.3 Experiments and rigs

3.3.1 Experiments in an anechoic room
3.3.2 Experiments in front of a vibrating plate
3.3.3 Experiment to measure a motor's noise

3.0 Experiments

3.1 Preparation of the membranes

3.1.1 Material

The material of the membrane is polyester. Its thickness is 10 micrometer and its surface density is about 10g/m^2. Its silver-grey surface can reflect the laser beam issued by the vibrometer.

3.1.2 Frame and adhesion

The shape of the membranes used in all the experiments is rectangular. The periphery of the membrane is adhered to a wooden frame.

Two adhesion methods are used, which give two different tension levels within the membrane.

The first method is to adhere the membrane completely to the frame along its periphery. By this method, the entire membrane is perfectly in a plan and the tension within the membrane is relatively high.

The second method is to adhere to the membrane partially to the frame along its periphery. By this method, the entire membrane is not perfectly in a plan and the tension within the membrane is lower than the fully adhered method.

.

3.1.3 Membrane with added mass

In order to reduce the effect of membrane's modes while measuring the acoustic wave, a "heavy" membrane compound was made, by adding mass between two membrane films. The mass is provided by adding paper tissue and water (Fig. 3.1). The heavy membrane compound is then adhered to the wooden frame.

The surface density of the heavy membrane is about 100g/m^2.

A B

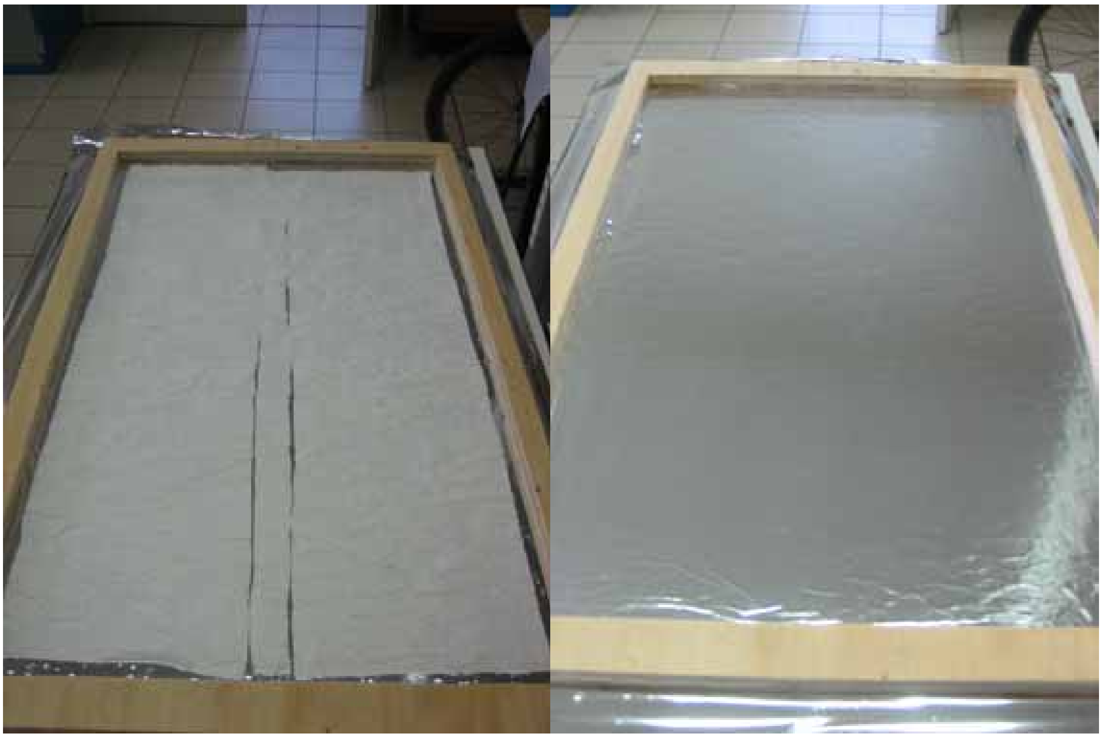

Figure 3.1 "Heavy" membrane realization A, Wet paper tissue is covered on the first membrane film. B, The second membrane film is then covered on the wet paper tissue

3.1.4 Conclusion on the membrane realizations

Two types of adhesion methods and two mass levels (light and heavy) can be used to make the membrane, so totally four different membranes are prepared for the experiments, they are:

- Light membrane, fully adhered to frame
- Light membrane, partially adhered to frame
- Heavy membrane, fully adhered to frame
- Heavy membrane, partially adhered to frame

Theoretically, the natural frequencies of a rectangular membrane fixed along its periphery can be calculated by the following equation [18]

$$f_{mn} = \frac{1}{2}\sqrt{\frac{\tau}{\rho_s}}\sqrt{\left(\frac{m}{l_x}\right)^2 + \left(\frac{n}{l_y}\right)^2} \qquad (3.1)$$

where τ is the membrane's tension per unite length, ρ_s is its mass per unite surface, l_x and l_y are the membrane's sizes.

In the extreme situations when the tension approaches to zero or the mass approaches to infinite, the membrane's nature frequency will be zero, the membrane will have no natural modes. Consequently, the heavier the membrane is or the higher its interior tension is, the more difficult its modes can be excited. This is why a heavy membrane was introduced to the experiment.

3.2 Data acquisition by the vibrometer

3.2.1 The vibrometer system

The laser acquisition and analysis system comprises four functional components.

- A Polytec OFV 056 Vibrometer Scanning Head (Fig. 3.2)
- A Polytec Junction Box
- A Polytec Vibrometer Controller
- A PC

To measure the velocity of the surface of an object, the Vibrometer Scanning Head issues a laser beam, which is reflected by the object and then received again by the Scanning Head. The reference signal is connected to the Jonction Box. The PC processes the received signal and the reference signal. The integrated FFT analyzer shows the measured velocity of the object in the frequency domain.

Figure 3.2 Polytec OFV 056 Vibrometer Scanning Head

3.2.2 Acquisition parameters

This part explains the acquisition parameters set for the vibrometer. These parameter settings will appear in the next part, for each of the experiments.

- Lx and Ly: The horizontal and vertical size of the acquisition region.
- N. of points in X and N. of points in Y: The numbers of discrete points in the two directions.
- Step in X and Y: Distance between two discrete points. The distance in X and in Y direction is identical. This is for the convenience of the further two dimensional spatial Fourier transform.
- Frequency range: The frequency range to be measured by the vibrometer. The span of the frequency range is Bandwidth.
- Sample frequency: The sample frequency is fixed by the system as

$$f_{sample} = 2.56 \times Bandwidth \tag{3.2}$$

This setting assures the Shannon theorem of data acquisition,

$$f_{sample} > 2 f_{\max} \tag{3.3}$$

where $f_{\max}$ is the maximum frequency component in the acquired data signal.

- Resolution: Frequency resolution of the acquisition.
- Average times: This is the average times for every measured point. By averaging the signal-to-noise ratio of spectra can be improved.
- Overlap: This is the permitted overlap between every two measure on one point. With this function, the time of measurement can be significantly reduced.
- Window: The Window is used to prevent data leakage. The Hanning window is the default setting.
- Reference: One or more reference must be used to determine the phase relations between different points. The reference can be dynamic (accelerometer) or acoustic (microphone).

3.3 Experiments and rigs

Three sets of experiments are carried out for different purposes.

3.3.1 Experiments in an anechoic room

The purpose of experiments in an anechoic room is to test the sound power calculated from membrane's measurements and compare it to the sound power measured by the microphone when the membrane is removed.

A loudspeaker located in one corner of he anechoic room issues a white noise. The membrane is suspended near the center of the room. The vibrometer is behind the membrane, located in another corner of the room (Fig 3.3). The loudspeaker, the membrane and the vibrometer are aligned in a line.

A microphone, which is in front of the membrane and is roughly in its geometry center, is used both as the reference of the vibrometer and as a pressure sensor for the sound power calculation.

The acoustic wave in the anechoic room can be considered as plan wave.

Four measurements are carried out with four different membranes. They are light membrane with full adhesion, light membrane with partial adhesion, heavy membrane with full adhesion and heavy membrane with partial adhesion, respectively.

To compare the sound power spectrum given by each membrane measurement and the sound power spectrum given by microphone, an additional measurement is carried out by moving the membrane away.

Fig 3.3 Rig in an anechoic room

The size of the membrane is 0.57m high and 0.50m wide. The acquisition area is in the center of the membrane. The weight of the heavy membranes is 35.3g, its surface density being 123.9g/m^2.

The acquisition parameters are:

L_x	0.40m	Sample frequency	16.38kHz
L_y	0.45m	Resolution	4Hz
N. of points in X	29	Average times	30
N. of points in Y	33	Overlap	75%
Step in X and Y	0.0138m	Window	Hanning
Frequency range	0Hz - 6.4kHz	Reference	Microphone

Table 3.1 Acquisition parameters of experiments in an anechoic room

3.3.2 Experiments in front of a vibrating plate

An aluminum plate is vibrated by a vibration actuator mounted on one side of the aluminum plate, roughly in its geometric center. The membrane is suspended in front of the aluminum plate to measure the near field acoustic holography the vibrating modes of the plate.

The thickness of the aluminum plate is 3mm. The size of the plate is 104cm in width and 100cm in height. It is fixed on its upper part. The membrane is placed at distances of 1cm and 5cm to the plate, respectively (Fig 3.4).

The signal to excite the vibration actuator is a truncated white noise, generated by the vibrometer system and amplified by an amplifier before send to the vibration actuator.

An accelerometer, mounted on the same side of the plate as the vibration actuator being mounted, is used as the reference for the vibrometer.

Two membranes are used: the partially adhered light membrane and the partially adhered heavy membrane.

Four measurements are carried out with membranes place at 1cm in front of the plate and 5cm in front of the plate, with the light and heavy membranes, respectively.

A previous experiment was carried out to measure the same acoustic field, at 1cm in front of the plate, by a P-U sound intensity probe – Microflown.

The purpose of these experiments is then to evaluate the performance of different membranes in characterizing the radiated acoustic field by the plate. Results are compared with the result obtained by the Microflown measurement.

Another study is the exponential decay of the near field wave by comparing results in different distances to the plate.

Fig 3.4 Rig with a vibrating plate

The size of the membrane is 1.00m high and 0.60m wide. The size of the acquisition is 0.389m high and 0.43m wide. The acquisition area is in the center of the membrane and covers the vibration actuator. The weight of the heavy membranes is 50.0g, its surface density being 83.3g/m^2.

The acquisition parameters are:

L_x	0.43m	Sample frequency	10.24kHz
L_y	0.389m	Resolution	5Hz
N. of points in X	21	Average times	80
N. of points in Y	19	Overlap	75%
Step in X and Y	0.0204m	Window	Hanning
Frequency range	0Hz - 4kHz	Reference	Accelerator

Table 3.2 Acquisition parameters of experiments with a vibrating plate

3.3.3 Experiment to measure a motor's noise

The holography of noises issued by a working vehicle motor has been previously measured by microphone. A new measurement by membrane is carried out in order to get a higher spatial resolution, thus to increase the high frequency limit of the frequency domain analysis.

To motor, supported by a concrete base, is in the center of an anechoic room.

The membrane, heavy and fully adhered to its frame, is suspended in front of the motor, at the same distance where the microphone has been placed in previous measurement (Fig 3.5).

Fig 3.5 Rig of motor's noise measurement

The size of the membrane is 1.00m high and 0.60m wide. The size of the acquisition is 0.647m high and 0.50m wide. The acquisition area is in the center of the membrane and covers the main part of the motor, which issues noises. The weight of the membrane is 70g, its surface density being 116.6g/m^2.

The acquisition parameters are:

L_x	0.50m	Sample frequency	10.24kHz
L_y	0.647m	Resolution	5Hz
N. of points in X	34	Average times	15
N. of points in Y	44	Overlap	75%
Step in X and Y	0.0147m	Window	Hanning
Frequency range	0Hz - 4kHz	Reference	Accelerator & microphone

Table 3.3 Acquisition parameters of experiments to measure a motor's noise

4.0 Results

4.1 Results of the experiments with the vibrating plate

4.1.1 Measured velocity field by membrane and its pressure field
4.1.2 Filtered velocity field and its pressure field
4.1.3 Corrected velocity field and pressure field of a heavy membrane
4.1.4 Comparison with Microflown results
4.1.5 Validation of evanescent wave

4.2 Results in the anechoic room

4.3 Results of the motor's noise

4.0 Results

4.1 Results of the experiments with the vibrating plate

4.1.1 Measured velocity field and its pressure field

The measured velocities of the aluminum plate and at 1cm in front of the plate are compared.

Figure 4.1 shows the velocity of the vibrating surface of the plate, measured directly by the vibrometer. (Fig. 4.1)

For the velocity at 1cm in front of the plate, take the velocity measured by the light membrane, partially adhered to its frame.

Four typical frequencies are selected, they are

- 50Hz: A nature frequency of the plate, the mode has a strip character.
- 220Hz: A nature frequency of the plate, the mode has a strip character.

- 610Hz: The mode of the plate starts to transit from a strip form to a circular form.
- 3500Hz: The mode of the plate is completely in a circular form.

Images of velocity (Fig. 4.2) show that in near field, vibrating modes of the aluminum plate can be captured by the membrane, at low and high frequencies.

However, artifacts exist in the images. One cause of the artifacts is the limit of spatial resolution (about 2cm). No higher resolution has been taken, for the reason that the results from membrane measurement will be compared with the results from hotwire measurements with the same spatial resolution.

Pressure fields (Fig. 4.3) at different frequencies were calculated based on measured velocity fields. At low frequencies, the modes can be seen in the pressure field. However, in high frequency, the propagation phenomena cannot be illustrated by the pressure field.

Notice that the images given here only represent the vibrating modes of the plates. Quantitative analysis will be discussed in next part, when the results are compared with results from a hotwire measurement of the same vibrating plate.

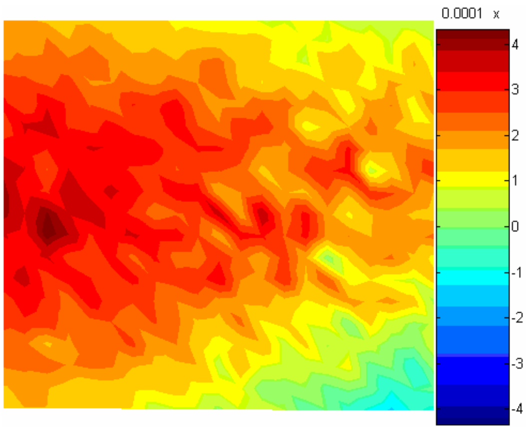

50Hz

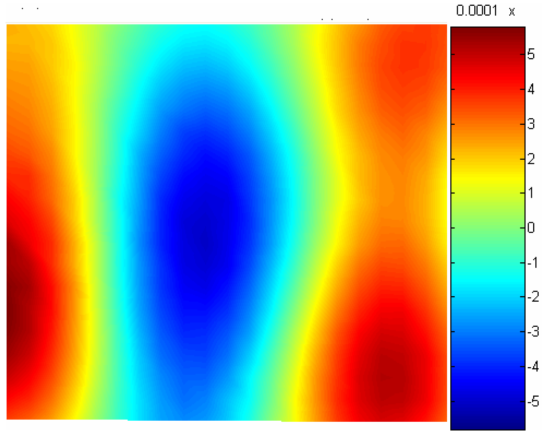

220Hz

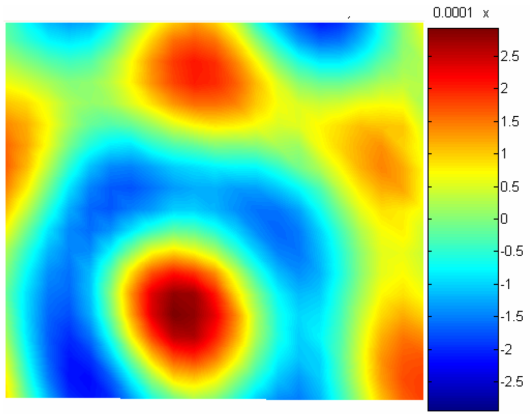

610Hz

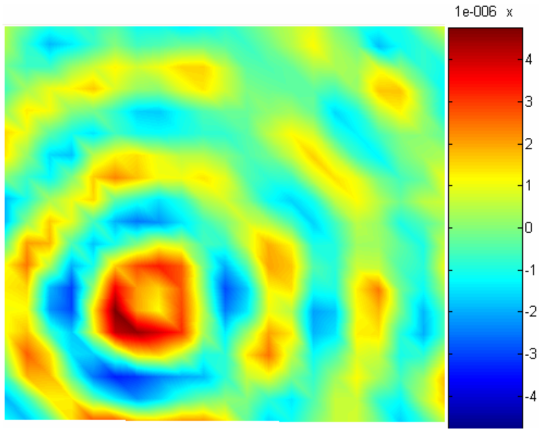

3500Hz

Figure 4.1 Velocity field measured of the aluminum plate, measured by the vibrometer. Frequencies are 50Hz, 220Hz, 610Hz, 3500Hz

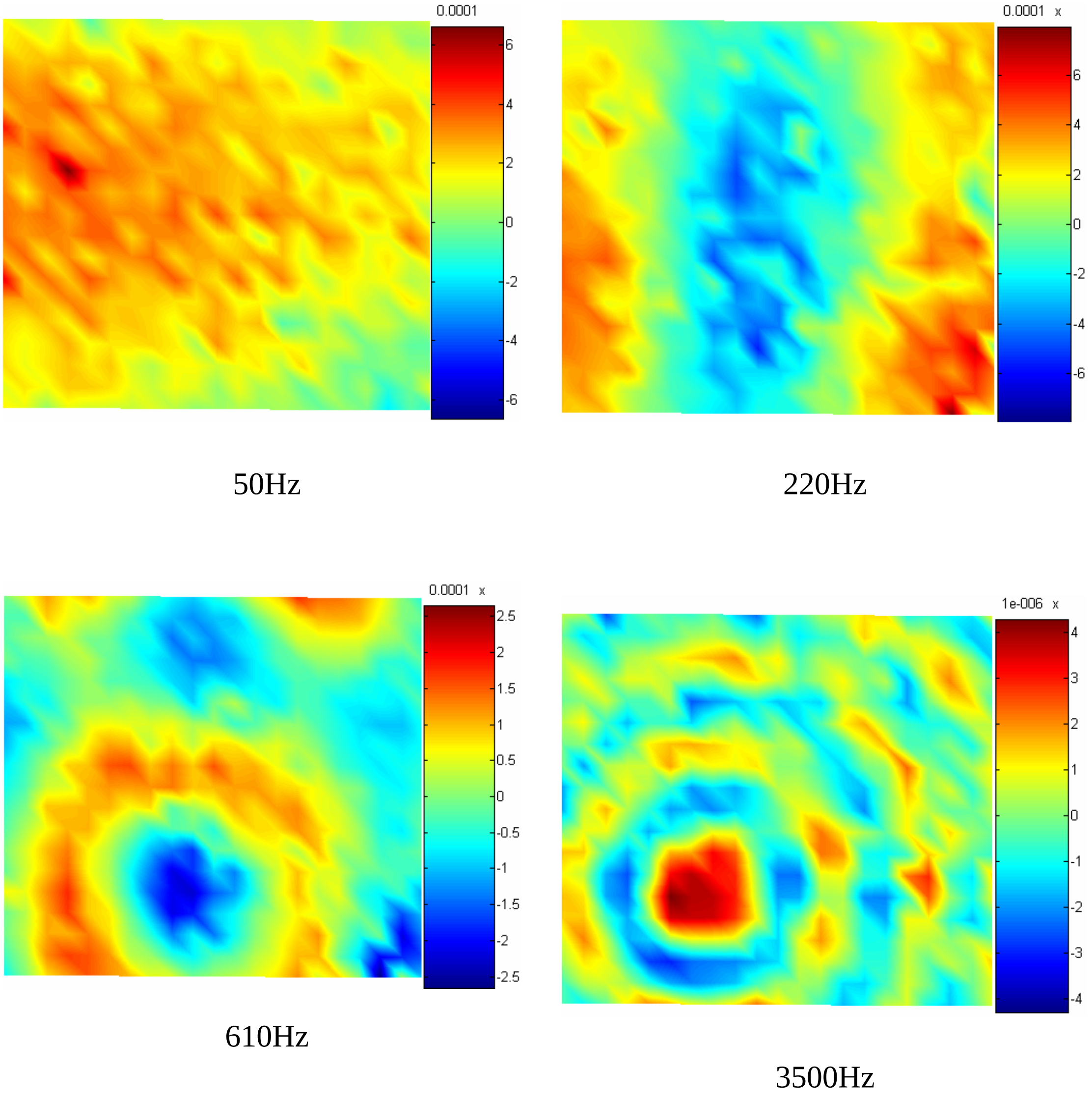

Figure 4.2 Velocity field measured by a light, partially adhered membrane, 1cm in front of a vibrating plate. Frequencies are 50Hz, 220Hz, 610Hz, 3500Hz

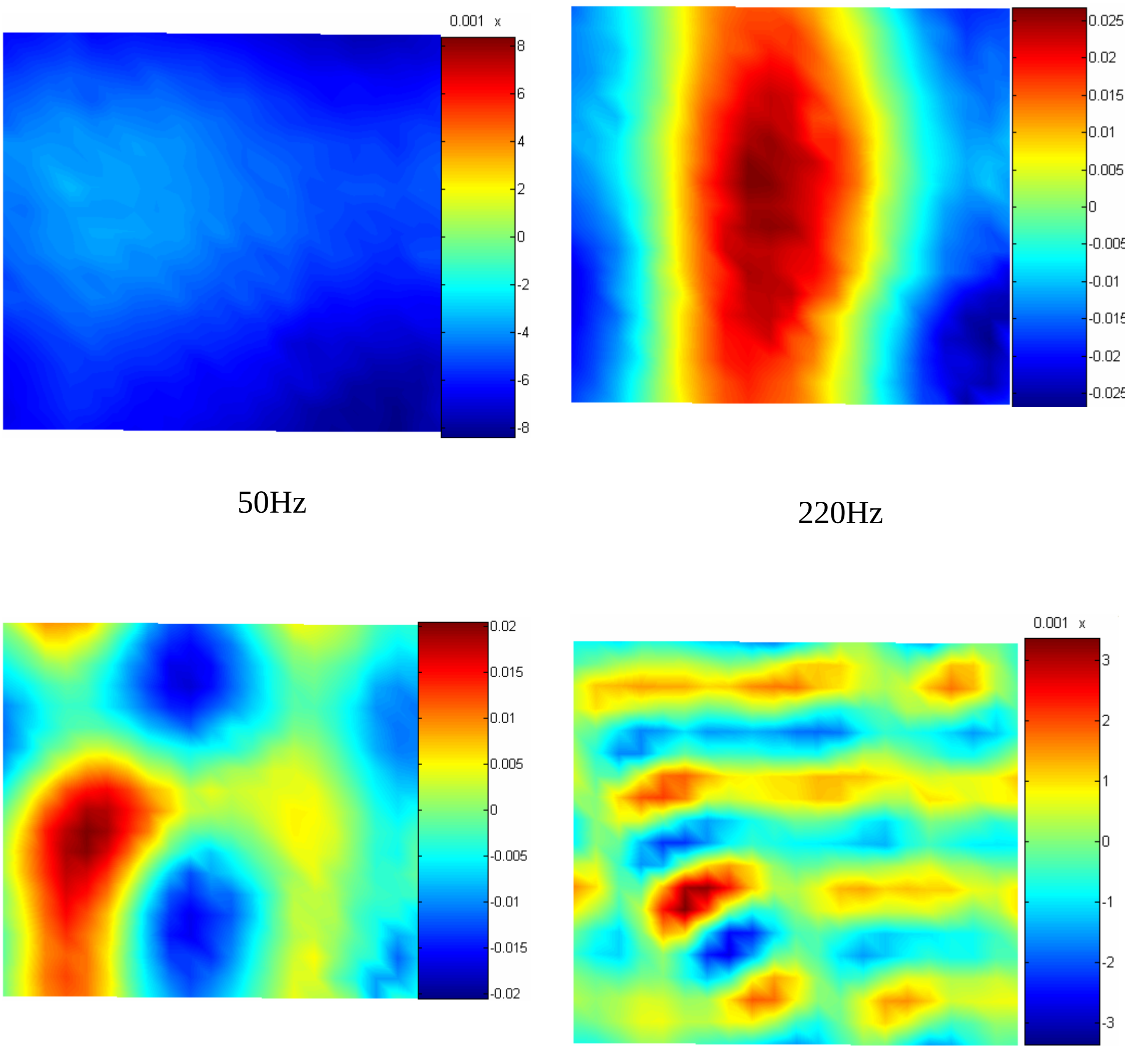

50Hz

220Hz

610Hz

3500Hz

Figure 4.3 Calculated pressure field based on the velocity field measured by a light, partially adhered membrane, 1cm in front of a vibrating plate. Frequencies are 50Hz, 220Hz, 610Hz, 3500Hz

4.1.2 Filtered velocity field and its pressure field

A filter was applied to the above velocity in order to reduce the artifacts.

The technique, explained previously, consists of eliminating the short wave length components.

$$\overline{v}^{*}(x,y)=\sum_{m=0}^{M-1}\sum_{n=0}^{N-1}\tilde{v}_{mn}^{*}e^{j2\pi mx/l_x}e^{j2\pi ny/l_y} \tag{4.1}$$

where

$$\tilde{v}_{mn}^{*}=\begin{cases}0,(\lambda_{mn}<L)\\ \tilde{v}_{mn},(\lambda_{mn}>L)\end{cases} \tag{4.2}$$

In this particular problem, the size of the acquisition area is 0.43m by 0.387m. The numbers of acquisition points are 21 by 19. The mesh step is 0.0205m.

L in equation (4.1) depends on frequency range. Based on observation on the results with different L, the value of L was finally determined as: L equals to 5 mesh steps (0.1024m) for the frequency range 0Hz – 250Hz, 3 mesh steps (0.0614m) for the frequency range 255Hz – 500Hz and 1 mesh step (0.0614m) for the frequency range 505Hz – 100Hz. For frequencies greater than 1000Hz, no filter is applied.

In both of the velocity (Fig. 4.4) and pressure (Fig. 4.5) images, the acoustic fields are smoothed, presenting fewer artifacts. However, once more, as frequency increase – at 610Hz, the pressure field is slightly deformed from the velocity field.

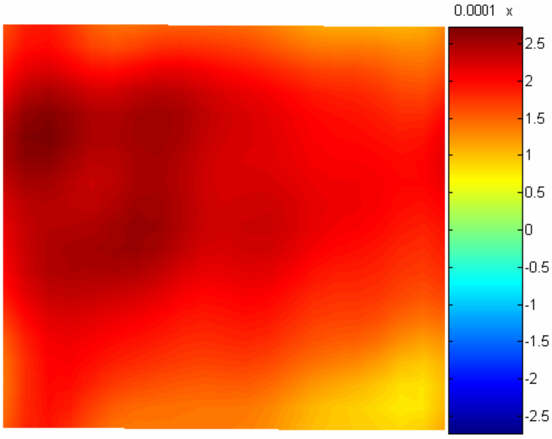

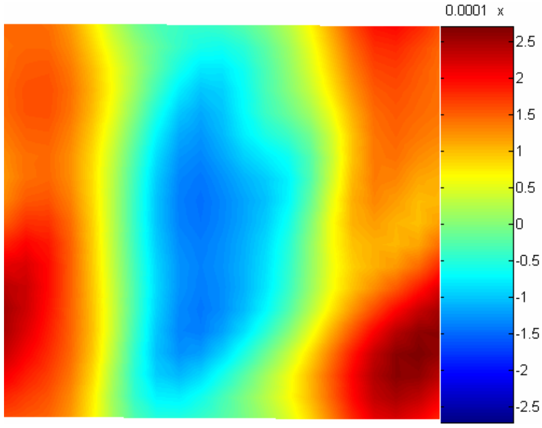

220Hz

50Hz

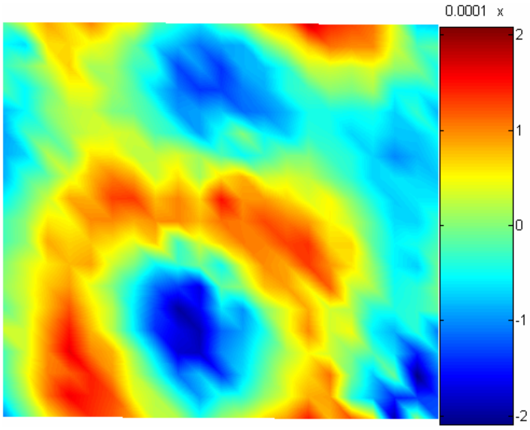

610Hz

Figure 4.4 Filtered velocity field measured by a light, partially adhered membrane, 1cm in front of a vibrating plate. Frequencies are 50Hz, 220Hz and 610Hz

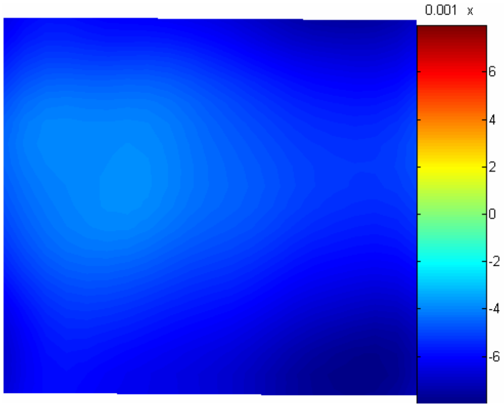

50Hz

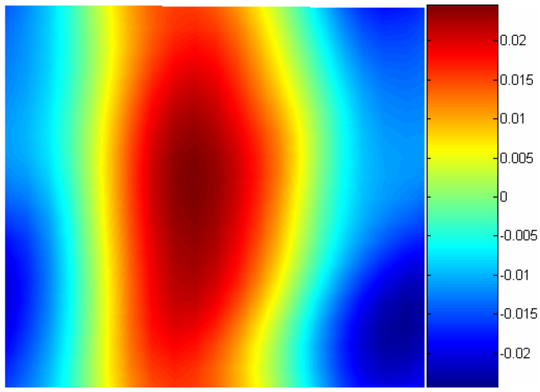

220Hz

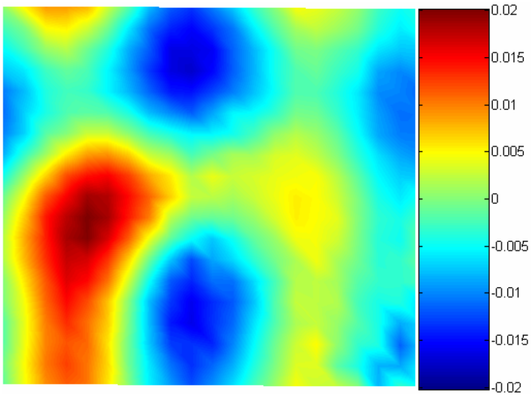

610Hz

Figure 4.5 Calculated pressure field based on the filtered velocity field measured by a light, partially adhered membrane, 1 cm in front of a vibrating plate. Frequencies are 50Hz, 220Hz and 610Hz

4.1.3 Corrected velocity field and pressure field of a heavy membrane

For a heavy membrane, to estimate the real acoustic field without the presence of the membrane, the velocity field is mass corrected after being filtered. Take the results of the heavy membrane, partially adhered to its frame, 1cm in front of a vibrating membrane.

Four typical frequencies are selected, they are

- 50Hz: A nature frequency of the plate, the mode has a strip character.
- 220Hz: A nature frequency of the plate, the mode has a strip character.
- 610Hz: The mode of the plate starts to transit from a strip form to a circular form.
- 3500Hz: The mode of the plate is completely in a circular form.

Vibrating modes and propagation phenomena can be observed in the mass corrected velocity (Fig. 4.6) and pressure (Fig. 4.7) fields in both low frequency range and high frequency range. However, in low frequency and intermediate frequency range, deformations are observed.

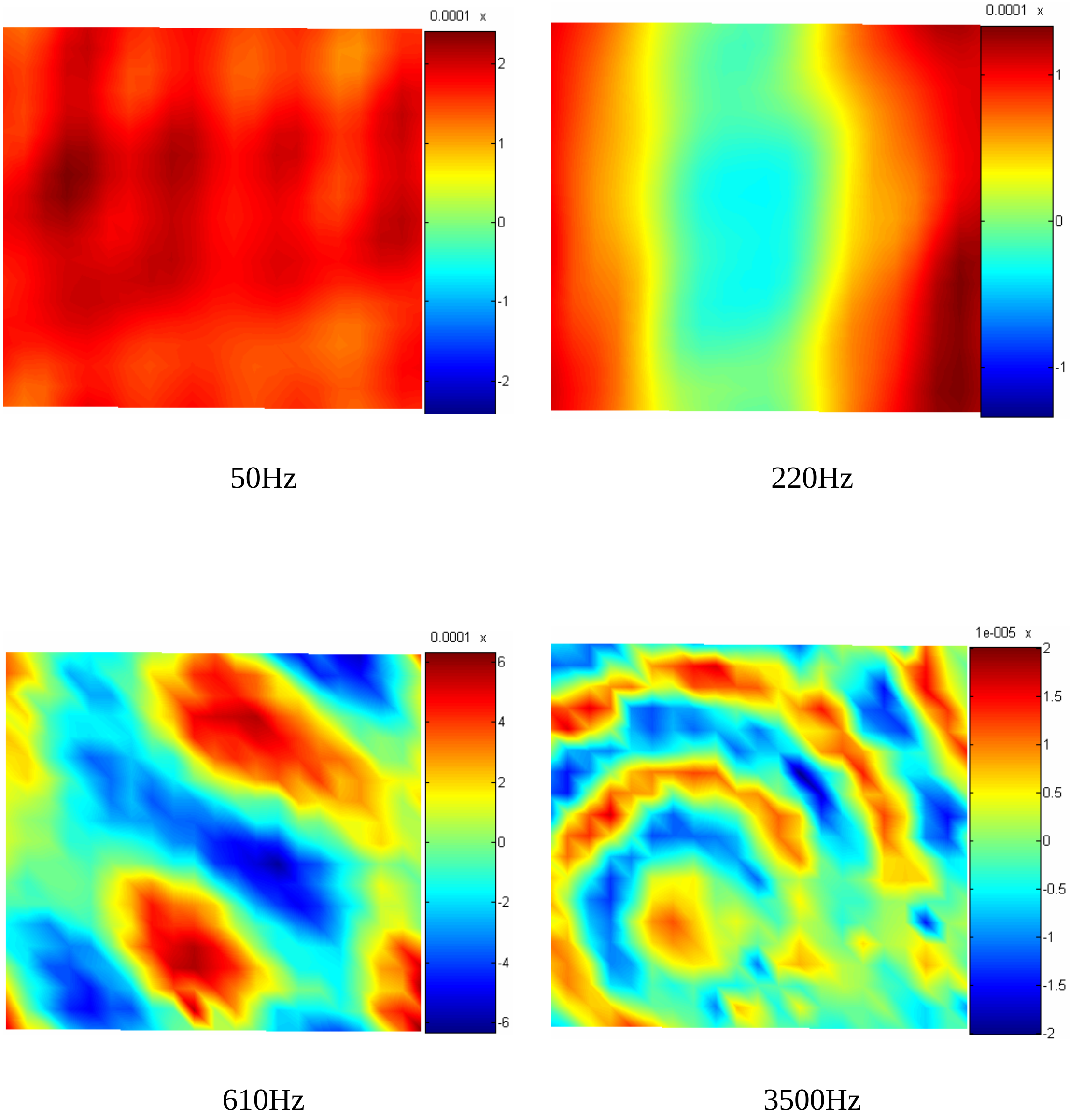

Figure 4.6 Mass corrected velocity field measured by a heavy, partially adhered membrane, 1cm in front of a vibrating plate. Frequencies are 50Hz, 220Hz, 610Hz and 3500Hz

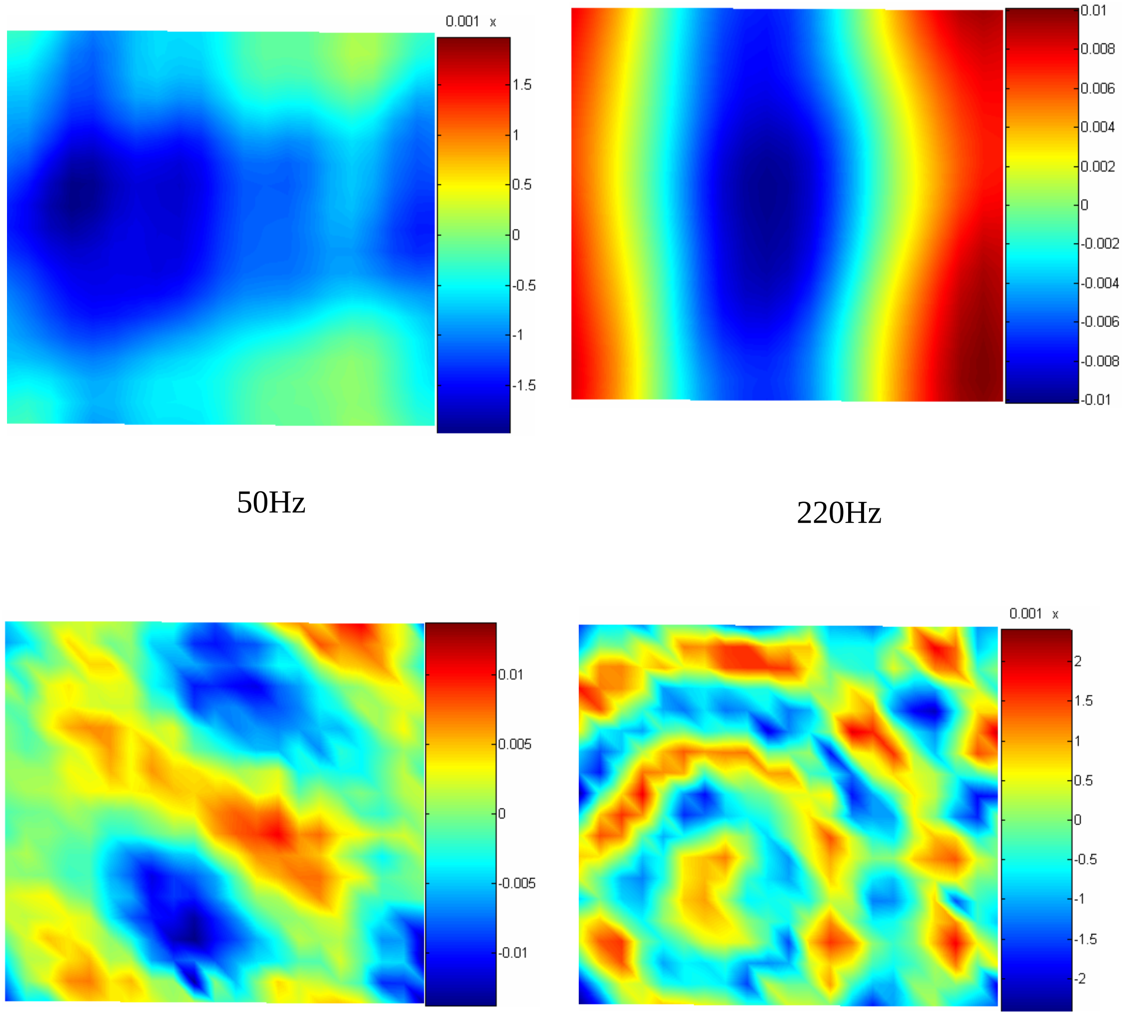

50Hz 220Hz

610Hz 3500Hz

Figure 4.7 Mass corrected pressure field based on the filtered velocity field measured by a heavy, partially adhered membrane, 1 cm in front of a vibrating plate. Frequencies are 50Hz, 220Hz, 610Hz and 3500Hz

4.1.4 Comparison with Microflown's results

A previous experiment by Microflown approach was carried out to measure the acoustic particle velocity field, 1cm in front of the same aluminum plate.

The acquisition parameters of the two measurements are the same, except that the positions of the vibration actuator are slightly different. Figure 4.8 shows the comparison of measured velocity fields in two different frequencies, by the Microflown method and the membrane method. The membrane is a light membrane, partially adhered.

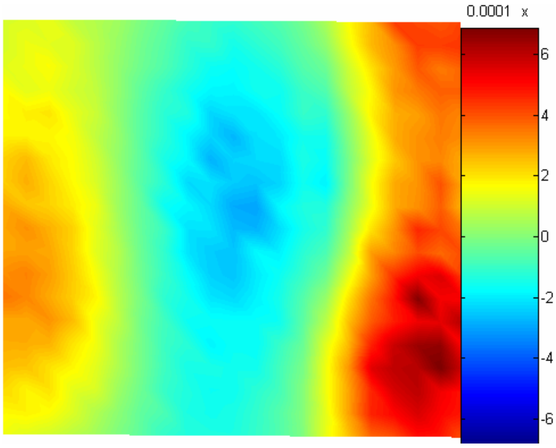

Microflown 220Hz

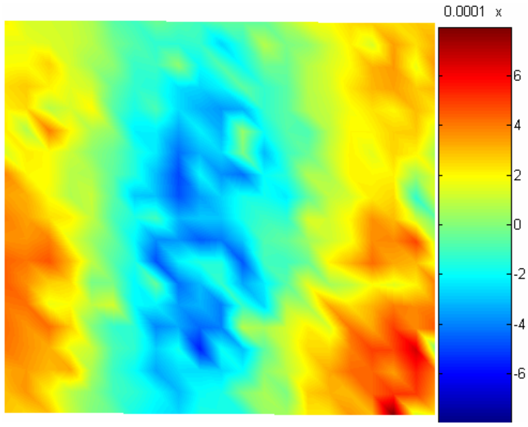

Membrane 220Hz

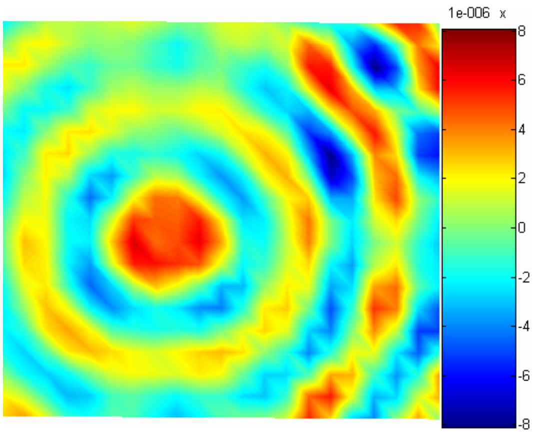

Microflown 3500Hz

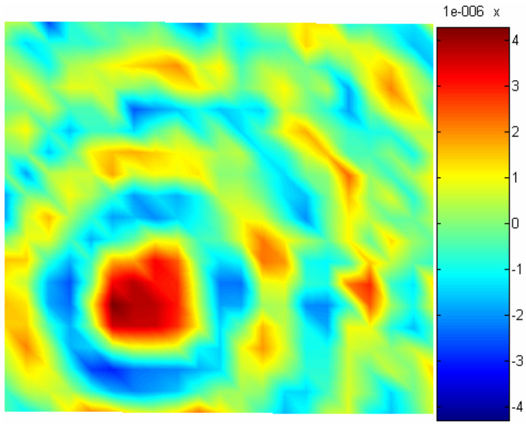

Membrane 3500Hz

Figure 4.8 Comparison between Velocity fields measured by Microflown and Membrane measurements.

4.1.5 Validation of evanescent wave

In chapter 2, the notion of propagative and evanescent wave has been introduce. The property of propagative or evanescent character is determined by the reduce wave number k_{mn}^{z}.

In the plate vibrating experiment, the calculation of k_{mn}^{z} with different frequencies shows that the acoustic waves have a strong evanescent character. The propagating part of acoustic waves are only associated with a few of small value (m, n) indexes.

Velocity field at 5cm from the plate can be calculated from the velocity field at 1cm from the plate. The theory has been explained in chapter 2 (Evanescent wave).

By comparing the filtered velocity measured by light membrane at these two distances, the acoustic wave shows a strong evanescent character: The velocity decreases as distance increases. (Fig. 4.9 A and C)

Based on the measured velocity at 1cm, velocity at 5cm is predicted. (Fig. 4.9 B). This result show good agreements with the measured result (Fig. 4.9 C)

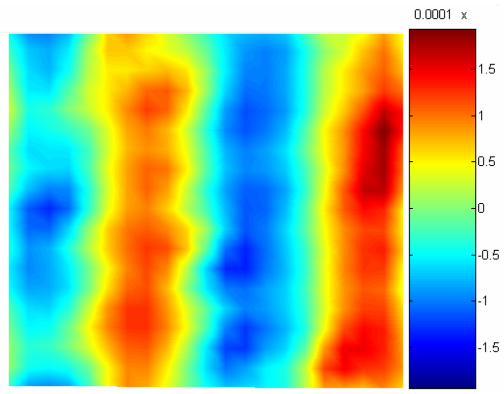

(A) Filtered velocity of light membrane, 1cm in front of plate, at 490Hz

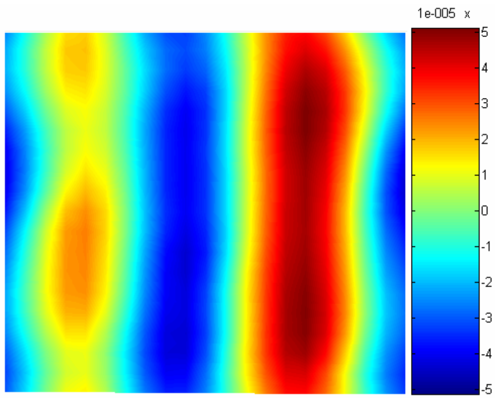

(B) Predicted velocity 5cm in front of membrane, based on (A), at 490Hz

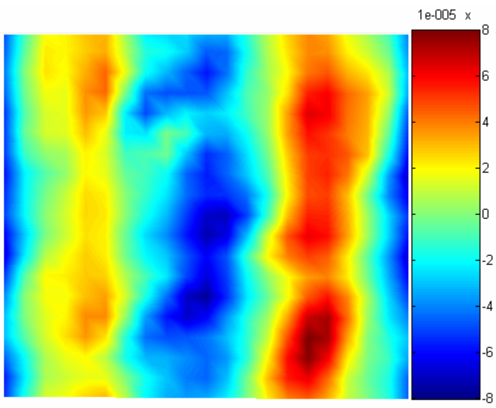

(C) Filtered velocity of light membrane, 5cm in front of plate, at 490Hz

Figure 4.9 Validation of evanescent wave Velocity at 1cm is at the order of 10^{-4} and velocity at 5cm is at the order of 10^{-5}

4.2 Results in the anechoic room

Sound power spectrum measured by a microphone, in front of the membrane is compared with sound power calculated by membrane measurements.

For light membranes, sound power is calculated based on the filtered velocity and pressure. For heavy membranes, sound power is calculated based on mass corrected velocity and pressure. Sound powers are compared in dB level (Fig. 4.10).

In low frequency range, results of the four different membranes give good estimations of the real sound power. As frequency rises, the gaps between microphone's results and membrane's results become greater. However, the forms of the curves given by membranes and by microphone are coherent. Results of light membranes have smaller gaps to microphone measured results, compared to heavy membranes.

Differences between results of fully adhered and partially adhered membranes are small.

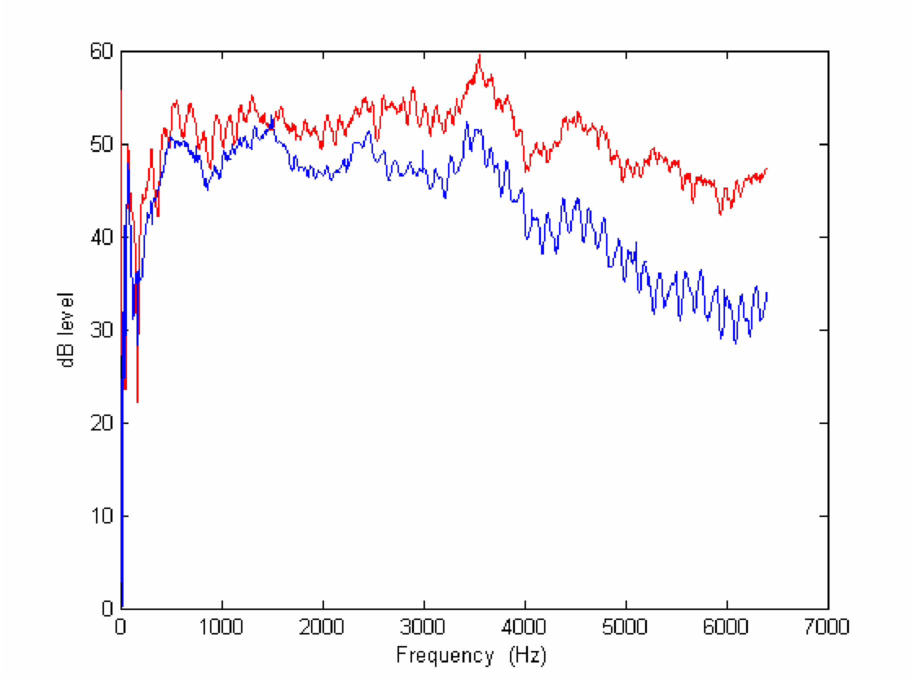

(A) Light membrane, fully adhered.

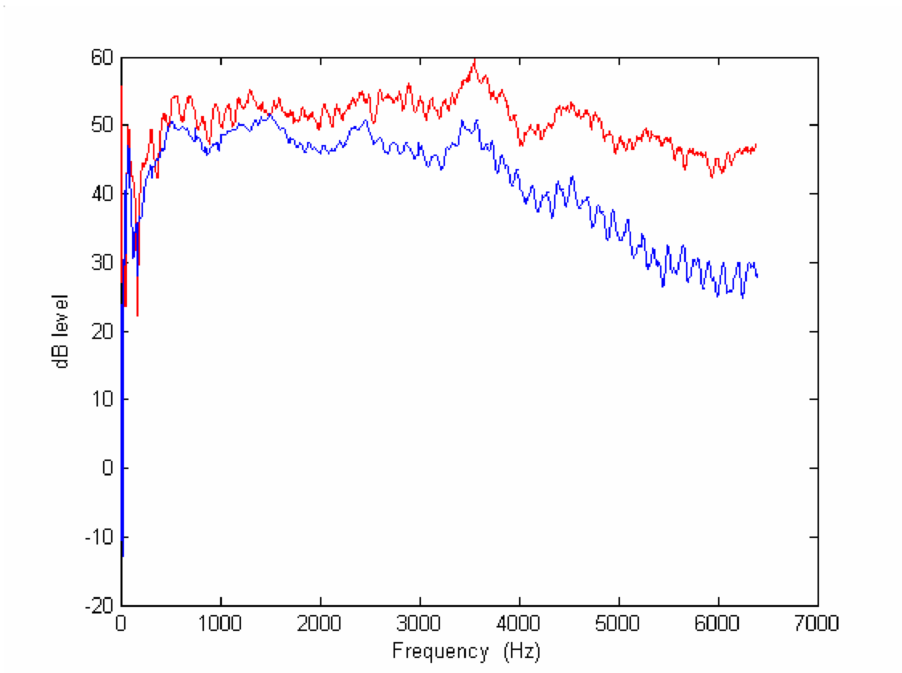

(B) Light membrane, partially adhered.

Figure 4.10 (1) Comparison of sound power of microphone and membranes in anechoic room Red curve: microphone's result. Blue curve: membrane's result.

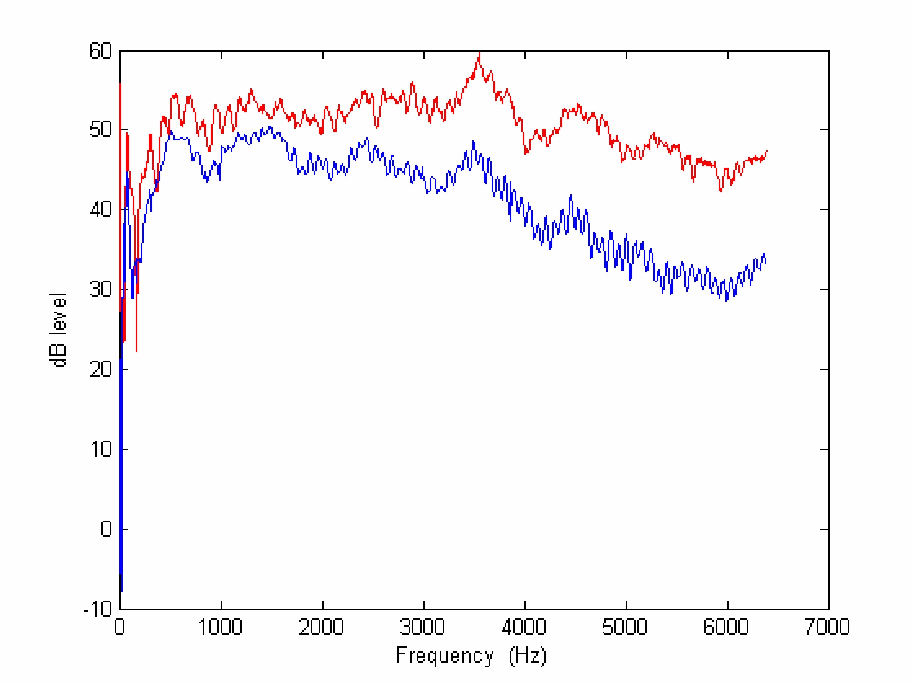

(C) Heavy membrane, fully adhered.

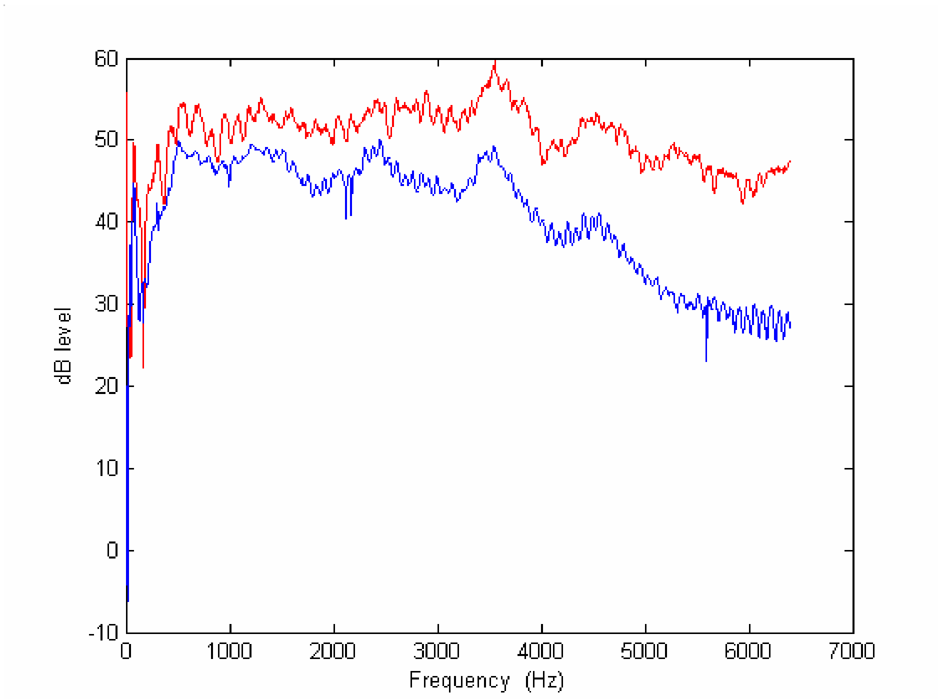

(D) Heavy membrane, partially adhered.

Figure 4.10 (2) Comparison of sound power of microphone and membranes in anechoic room Red curve: microphone's result. Blue curve: membrane's result.

4.3 Results of the motor’s noise

Pressure fields (mass corrected) of the motor’s noise are compared with previous results by microphone measurement under the same condition. (Fig. 4.11)

Mesh of microphone measurement is 6 by 9; mesh of membrane measurement is 33 by 44.

Below 800Hz, images of pressure by membrane measurement are not representative because of too much artifact exists.

At frequencies 800Hz, 1200Hz, 1820Hz. The comparison of pressure fields shows coherence between two measurements. However, results obtained by membrane show more artifacts than results obtained by microphone.

For frequencies greater than 2000Hz, the results of microphone measurement are no longer representative because of it low spatial resolution.

(A) 800Hz

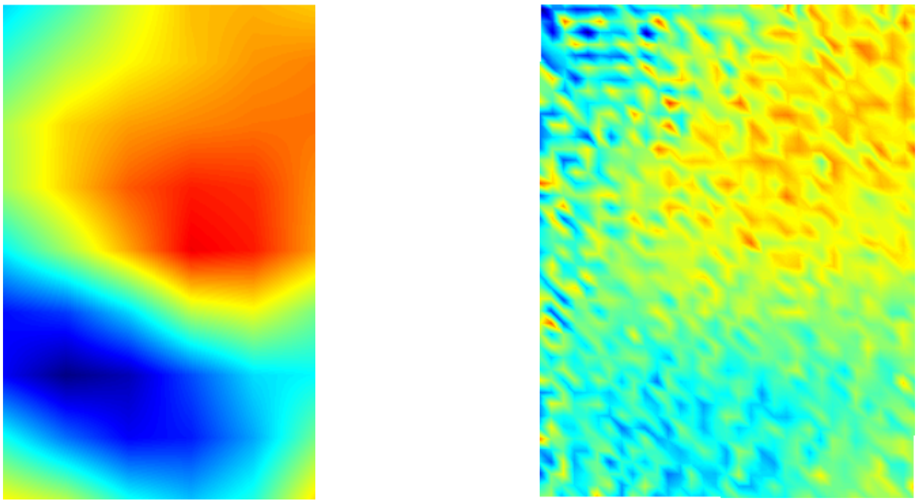

(B) 1200Hz

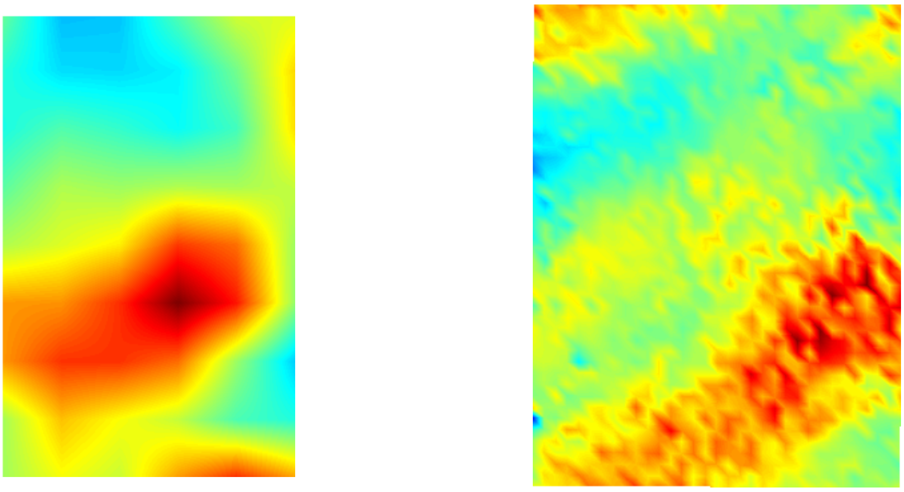

(C) 1820Hz

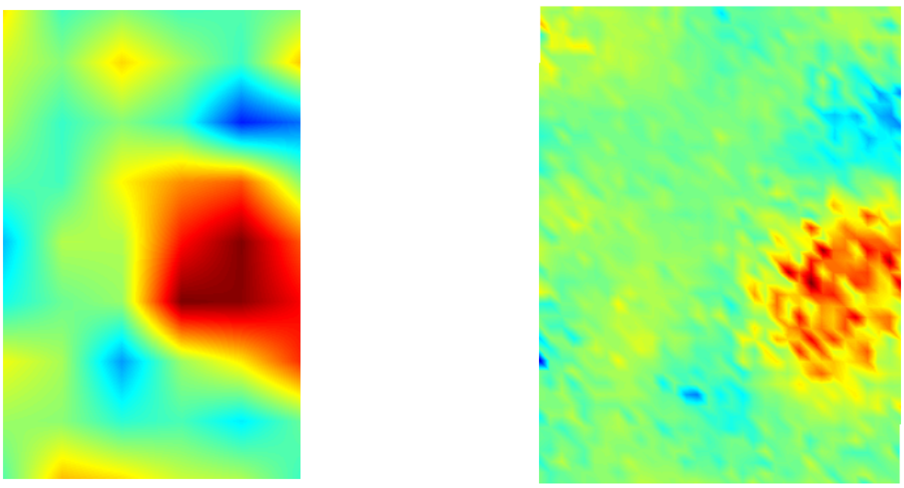

Figure 4.11 Comparison of motor's acoustic pressure field by microphone and membrane measurement.

5.0 Discussions

5.1 Evaluations of the results

5.2 Recommended future works

5.0 Discussions

5.1 Evaluations of the results

The main advantages of the method of membrane’s measurement presented in this project are firstly its high spatial resolution and secondly its ease to realize.

The main difficulty of this method is that artifacts in the measure acoustic field are hard to reduce, though a filter technique has been applied. A fundamental reason for this is that the membrane governing equation adopted in the theory cannot describe the exact behavior of the real membrane, particularly for the interior tension of the membrane.

Nevertheless, the forms of the measured velocity fields in various experiments agree with results obtained by conventional approaches.

For a heavy membrane, acoustic pressure obtained on the basis of the mass correction theory developed in chapter 2 shows good estimations of the results obtained by conventional approaches. However, acoustic pressure obtained with a light membrane cannot illustrate the theoretically predicted pressure field in high frequency range, thus is only available in low frequency range.

In terms of acoustic power, experiments in the anechoic room show that acoustic power estimated by membrane measurement is inferior to the microphone measured results; however spectrums show that the acoustic power in frequency distribution agrees with the microphone’s result.

5.2 Recommended future works

1. Better realization of the membrane: Reduce interior tension while keep the surface of the membrane in on plane.

2. Further studies on the mechanical behavior of the membrane in acoustic field.

3. Numerical treatment to reduce the artifacts in the acoustic field measured by the membrane.

6.0 References

1. Victor I. Neeley. *Acoustical Holography*. **Automotive Engineering Congress Detroit**, Mich. January 10-14, 1972

2. Andrews N. Norris, *Far-field acoustic holography onto cylindrical surfaces using pressure measured on semicircles* **J. Acoust. Soc. Am**., Vol. 102, No. 4, October 1997

3. E. G. Williams, *Imaging the sources on a cylindrical shell from far-field pressure measured on a semicircle,* **J. Acoust. Soc. Am**. 99, 2022–2032~1996

4. J. D. Maynard, E. G. Williams, and Y. Lee. *Nearfield acoustic holography: I. Theory of generalized holography and the development of NAH*. **The Journal of the Acoustical Society of America** -- October 1985 -- Volume 78, Issue 4, pp. 1395-1413

5. R. Steiner and J. Hald, *Near-field acoustical holography without the errorsand limitations caused by the use of spatial DFT* **Int. J. Acoust. Vib**.6, 83–89 2001

6. J. Hald. *Patch near-field acoustical holography using a new statistically optimal method*. **Inter-noise 2003**, Jeju International Convention Center, Seogwipo, Korea, 2003-08-25–2003-08-28.

7. R. Scholte, N.B. Roozen, *High resolution near-field acoustic holography,* **Proceedings of the Eleventh International Congress on Sound and Vibration**, 5-8 July 2004, St. Petersburg 2004

8. Gajendra Shekhawat and Vinayak P. Dravid. *Near-Field Acoustic Holography as a High Resolution Sub-Surface Imaging System on Scanning Probe Microscopy Platform: Seeing the Invisible* **Microsc Microanal** 11(Suppl 2), 2005

9. Jacob Franden *Handbook of Modern sensors Physics,* Designs and Applications **AIP Press** 1997

10. F. Jacobsen. *A note on finite difference estimation of acoustical particle velocity*. **J. Sound Vib**., 256(5):849-859, 2002

11. de Bree, H.-E.; Leussink, P.; Korthorst, T.; Jansen, H.; Lammerink, T.; Elwenspoek, M. *A Novel Device Measuring Acoustical Flows Solid-State Sensors and Actuators*. **1995 and Eurosensors IX. Transducers apos; 95. The 8th International Conference** on Volume 1, Issue , 25-29 Jun 1995 Page(s):536 - 539

12. F. Jacobsen and H-E de Bree. *Measurement of sound intensity: p-u probes versus p-p prbes*. **In Proceedings of NOVEM** 2005

13. Sound fields at a glance, Localisation and analysis of sound sources and acoustic weak points with new measurement technique **www.ibp.fhg.de/akustik**

14. Finn Jacobsen and Yang Liu. *Near field acoustic holography with particle velocity transducers*, **J. Acoust. Soc. Am.**, Vol. 118, No. 5, November 2005

15. Finn Jacobsen and Yang Liu, *Near Field Acoustic Holography Based on an Array of Particle Velocity Sensors,* **The 2005 Congress and Exposition on Noise Control Engineering** 07-10 Aug 2005 Rio de Janeiro Brazil

16. Q. Leclère, B. Laulagnet *Particle velocity field measurement using an ultra-light membrane* **Applied Acoustics**

17. Christopher H.M. Jenkins and Umesh A. Korde. *Membrane vibration experiments: An historical review and recent results*. **J. Sound Vib.**, 78(4):1395-1413, 2006

18. Jacques Jouhaneau. *Notion élémentaires d'acoustique 2^e^ édition, Electroacousticque*. **Technique & Documentation –** 2000